Frontiers in Bioscience Landmark

Front. Biosci. (Landmark Ed) **2022**; 27(6): 184
https://doi.org/10.31083/j.fbl2706184

Original Research

PINK1/Parkin-Mediated Mitophagy Plays a Protective Role in Albumin Overload-Induced Renal Tubular Cell Injury

Pengpeng Duan[1,†], Jin Tan[1,†], Yuyang Miao[1], Qiang Zhang[1,*]

[1]Department of Geriatrics, Tianjin Medical University General Hospital, Tianjin Geriatrics Institute, 300052 Tianjin, China
*Correspondence: zhangqiangyulv@163.com (Qiang Zhang)
† These authors contributed equally.
Academic Editor: Mateusz Maciejczyk
Submitted: 5 April 2022 Revised: 28 May 2022 Accepted: 28 May 2022 Published: 7 June 2022

Abstract

Background: Proteinuria is an important symptom of chronic kidney disease irrespective of its initial pathogenesis. Mitochondrial dysfunction is an early pathophysiological event in proteinuria-induced tubular damage. Mitophagy, the selective degradation of damaged mitochondria targeted by autophagy, contributes to mitochondrial homeostasis and is primarily regulated by the PTEN-induced kinase 1 (PINK1)/Parkin pathway. In this study, we evaluated the function of mitophagy in proteinuria-induced tubular injury and mechanism. **Methods**: HK-2 cells were transfected with Parkin siRNA or Parkin overexpression plasmids for 48 h followed by treatment with albumin (8 mg/mL) for 8 h. JC-1 staining, ATP detection, and reactive oxygen species (ROS) detection were used to determine mitochondrial function. Immunoblot, LC3/mitochondria co-localization analyses, and Mito-Keima were employed to detect mitophagy. Immunoblot analysis and TUNEL were used to detect apoptosis. **Results**: Albumin overload induced mitochondrial dysfunction and mitophagy activation in HK-2 cells. Parkin knockdown inhibited albumin overload induced-mitophagy. Parkin overexpression further upregulated albumin overload induced-mitophagy. Parkin deficiency aggravated albumin overload-induced mitochondrial dysfunction and the overproduction of ROS, resulting in increased cell injury. Contrarily, Parkin overexpression helped maintain mitochondrial function and attenuate ROS generation, contributing to cell protection. **Conclusions**: Our results suggest that by clearing damaged mitochondria and maintaining mitochondrial function, PINK1/Parkin-mediated mitophagy contributed to tubular cell survival during albumin overload. PINK1/Parkin-mediated mitophagy may be a potential therapeutic target for proteinuria in tubular epithelial cells.

Keywords: renal tubular epithelial cell; proteinuria; mitochondrial dysfunction; mitophagy; PINK1; Parkin

1. Introduction

Proteinuria is an important symptom of most chronic kidney diseases, including nephrotic syndrome and diabetic nephropathy [1]. Although proteinuria results from glomerular injury, it is also commonly recognized as an independent component that leads to renal tubular lesions, which exacerbate kidney injury and renal function loss [2]. In recent decades, a number of reports have confirmed some pathological changes of proteinuria-associated renal injury, including interstitial fibrosis, inflammatory response, and tubular cell injury and death [3–6]. It is critical to understand the mechanisms behind these pathologic changes for developing effective therapies against proteinuric nephropathy.

Mitochondria are essential for maintaining the high energy demands renal tubular cells, as well as controlling cell death and various signaling cascades [7,8]. Accumulation of albumin in tubular cells, a major urinary protein component, can induce mitochondrial damage, reactive oxygen species (ROS) accumulation, and mitochondria-dependent apoptosis, all of which strongly correlate with reduced renal function [5,9]. Thus, the timely removal of damaged mitochondria and the maintenance of their normal function may be an effective therapeutic strategy for preventing the renal tubular cell injury associated with albumin overload.

Mitophagy is a particular type of autophagy that selectively clears defective and excessive mitochondria, contributing to mitochondrial homeostasis and cell survival [10,11]. In mammalian cells, mitophagy necessitates a unique priming process to identify and flag the mitochondria destined for autophagic degradation, with current data identifying PTEN induced kinase 1 (PINK1)/Parkin-mediated mitophagy as the major regulatory mechanism for this process in response to cell stress. Under normal conditions, healthy mitochondria import PINK1 into the inner mitochondrial membrane where it is cleaved and proteolytically degraded [12]. However, when mitochondria are depolarized by various stressors, the import of PINK1 is suppressed, resulting in PINK1 accumulation on the outer mitochondrial membrane, and thus the recruitment and phosphorylation of Parkin [12,13]. Upon phosphorylation, Parkin ubiquitinates various proteins within the outer mitochondrial membrane, inducing and promoting their autophagic removal [14].

PINK1/Parkin-dependent mitophagy has been reported in many kinds of kidney diseases [15–17]. However, the involvement and function of PINK1/Parkin-dependent

mitophagy in albumin overload remains unclear and requires further evaluation. Given this, we designed this study to investigate the function of the PINK1/Parkin pathway in albumin overload-induced renal tubular cell damage by detecting its effects on mitophagy, mitochondrial function, ROS, and apoptosis.

2. Materials and Methods

2.1 Cells, Antibodies, and Special Reagents

The human proximal tubular epithelial cell line HK-2 was obtained from the American Type Culture Collection (ATCC), ATCC Cat# CRL-2190, RRID:CVCL_0302. The sources of the antibodies used in this study were as follow: anti-LC3B (Cell Signaling Technology, 2775), anti-LC3B (Novus, NB100-2220), anti-SQSTM1 (Abcam, ab109012), anti-Cleaved Caspase 3 (Sigma-Aldrich, AB3623), anti-GAPDH (Cell Signaling Technology, 2118), anti-PINK1 (Novus, BC100-494), anti-PARK2/Parkin (Cell Signaling Technology, 4211), anti-Tom20 (Santa Cruz Biotechnology, sc-17764), HRP-labeled Goat Anti-Rabbit IgG (Beyotime, A0208), HRP-labeled Goat Anti-mouse IgG (Beyotime, A0216), Alexa Fluor 488 (Thermo Fisher Scientific, A-21222). Human serum albumin (HAS/ALB) was purchased from Sigma Aldrich (St. Louis, MO, USA). Small interfering RNA (siRNA) targeting human Parkin, negative control siRNA, Parkin plasmids, and control empty plasmid vector were purchased from GenePharma (Shanghai, China). The sequences of siRNA oligonucleotides were sa follows: Parkin siRNA, 5′-CCUUCUGCCGGGAAUGUAATT; control siRNA, 5′-UUCUCCGAACGUGUCACGUTT.

2.2 Cell Culture, Treatment, and Transfection

Human proximal tubular epithelial HK-2 cells were grown in Dulbecco's modified Eagle's/F12 medium supplemented with 10% fetal bovine serum, 1% penicillin/streptomycin (all from Gibco, Gaithersburg, MD, USA), and human recombinant epidermal growth factor (10 ng/mL, Thermo Fisher Scientific) at 37 °C under 5% CO2. Human serum albumin was purchased from Sigma-Aldrich (St. Louis, MO, USA). Based on the results of our previous study, albumin overload experiments were performed by culturing HK-2 cells with 8 mg/mL albumin for 8 h [18]. Small interfering RNA (siRNA) targeting human Parkin, negative control siRNA, Parkin plasmids, and the control empty plasmid vector were purchased from GenePharma (Shanghai, China). Transfections were performed using Lipofectamine 3000 (Invitrogen, Carlsbad, CA, USA) following the manufacturer's instructions.

2.3 RNA Extraction and Real-Time Quantitative Polymerase Chain Reaction (RT-PCR)

Total RNA was extracted from cultured cells using the TRIzol® reagent (Invitrogen, Carlsbad, CA, USA) according to the manufacturer's instructions after 48 h of transfection. RNA concentrations were estimated by Nanodrop Spectrophotometer (Thermo Scientific, Waltham, MA, USA). Reverse transcription and qRT-PCR were performed using the Custom gene qRT-PCR Quantitation Kit (GenePharma, Shanghai, China) with specific primers. The sequences of the primers were: Parkin, forward: 5′-GGAGTGCAGTGCCGTATTTG-3′ and reverse: 5′-AGGGCTTGGTGGTTTTCTTGA-3′; GAPDH, forward: 5′-GGTGGTCTCCTCTGACTTCAA-3′ and reverse: 5′-GTTGCTGTAGCCAAATTCGTTGT-3′. The cycle threshold (Ct value) was detected by a CFX ConnectTM RT-PCR system (Bio-Rad). The relative quantity of mRNA transcripts was calculated using the $2^{-\Delta\Delta ct}$ method, and GAPDH was used as the endogenous control for normalization.

2.4 Immunoblot Analysis

Total proteins were extracted from HK-2 cells with a protein extraction kit (Promega, Madison, WI, USA) according to the manufacturer's protocol. Protein concentrations were examined using a BCA assay kit (Thermo, Waltham, MA) according to the manufacturer's instructions. The proteins were separated by 10% or 12% sodium dodecyl sulfate-polyacrylamide gel electrophoresis. Next, the proteins were transferred onto 0.22 μm polyvinylidene difluoride membranes (Merck Millipore, Burlington, MA) and blocked with 5% non-fat dry milk in Tris-buffered saline and Tween 20 for 2 h at room temperature. The membranes were then incubated with primary antibodies overnight at 4 °C and with the appropriate horseradish peroxidase (HRP)-conjugated secondary IgG for 1 h at room temperature. Finally, chemiluminescence was imaged in a Chemi DocTM XRS + WB molecular imager using Image LabTM software (Bio-Rad, Herculaes, CA, USA), and band intensities were quantified with ImageJ 1.8.0 software (National Institutes of health, Bethesda, MD, USA).

2.5 Detection of Mitophagy

Mitophagy was determined by the co-localization of autophagosomes and mitochondria. HK-2 cells cultured on coverslips were incubated with red-fluorescing Mito-Tracker Red (50 nM, C1035, Beyotime, Shanghai, China) for 15 min at 37 °C. After twice washing with PBS, these cells were fixed with 4% paraformaldehyde for 15 min at room temperature. Then they were incubated with 1% Triton X-100 for 10 min and blocked with 3% BSA buffer for 30 min. Subsequently, cells were incubated with an LC3 (1:100) antibody at 4 °C overnight and incubated with green fluorescence-labeled secondary antibody for 1 h at room temperature. Finally, 4, 6-diamidino-2-phenylindole (DAPI) (Invitrogen, Carlsbad, CA, USA) was used as a counterstain. Images were visualized using an OLYMPUS confocal microscope (Tokyo, Japan). For quantification, over 100 cells in each group were examined for co-localization of autophagosomes (green) with mitochondria

(red) to estimate the percentage of cells with mitophagosome formation.

2.6 Mito-Keima Assay

HK-2 cells were transfected with the mKeima-Red-Mito-7 (Addgene, 56018) plasmid using Lipofectamine 3000 for 40 h and then treated with 8 mg/mL albumin for another 8 h. Nuclei were counterstained with Hoechst 33342 (C1027, Beyotime, China). The cells were imaged using an OLYMPUS confocal microscope (Ex = 550 nm, Em = 620 nm for acidic red fluorescence, Tokyo, Japan). For quantification, more than 20 cells in each group were examined for autolysosome formation to estimate the autolysosome dots/cell.

2.7 Detection of Mitochondrial Membrane Potential ($\Delta\psi m$)

$\Delta\psi$m was detected using a JC-1 assay kit (C2003S, Beyotime, China). After the indicated treatments, HK-2 cells cultured in 6-well plates were then washed with PBS and incubated with 1 ml JC-1 staining solution (5 μg/mL) at 37 °C for 20 min. Subsequently, HK-2 cells were washed twice with JC-1 buffer solution, and a fresh medium was added for detection. Images were captured captured using an AXIO Observer D1 fluorescence microscope (Carl Zeiss, Oberkochen, Germany) and were analyzed with ImageJ software to obtain the mean densities of the regions of interest, which were normalized to those of the control group. In cells with high mt$\Delta\Psi$, JC-1 aggregates in the mitochondria and gives off a red fluorescence. In cells with low mt$\Delta\Psi$, the JC-1 fails to aggregate in the mitochondria and remains in the cytoplasm in its monomer form, which exhibits green fluorescence. The value of mt$\Delta\Psi$ was expressed as the ratio of red/green fluorescence intensity.

2.8 Detection of ATP

Intracellular ATP levels were detected using an ATP assay kit (S0026, Beyotime, China). After indicated treatments, HK-2 cells cultured in 6-well plates were washed twice with PBS and lysed with ATP Cell Lysis solution in an ice bath. Then, the cell lysates were centrifuged at 12,000 $\times$ g for 5 min at 4 °C, and supernatants were collected. In a 96-well culture plate, 20 μL of each supernatant was mixed with 100 μL of ATP detection working dilution. Relative luminescence was assessed using a Varioskan LUX microplate reader (Thermo Scientific, Waltham, MA, USA). The standard curve for the quantification was prepared each time. ATP content was normalized by protein.

2.9 Detection of Intracellular ROS

HK-2 cells were incubated in 10 μM of the oxidation-sensitive fluorescent probe, 2,7-dichlorodihydrofluorescein diacetate (DCFH-DA) (S0033S, Beyotime) at 37 °C for 30 min, then washed with serum-free medium three times. Fluorescent images were photographed using a fluorescence microscope. The multifunctional microplate reader detected ROS levels at the $\sim$485/528 nm wavelength.

2.10 Detection of Mitochondrial ROS

HK-2 cells were incubated in 5 μM MitoSOXTM Red (M36008, Invitrogen, Carlsbad, CA, USA) at 37 °C for 10 min, and then washed with warm buffer three times. Images were photographed using a fluorescence microscope. The multifunctional microplate reader detected ROS levels at the $\sim$510/580 nm wavelength.

2.11 Analysis of Cell Apoptosis

Apoptosis was determined using a terminal deoxynucleotidyl transferase dUTP nick-end labeling (TUNEL) apoptosis assay kit (C1088, Beyotime, China). HK-2 cells cultured on coverslips were washed with ice-cold PBS and subsequently fixed with 4% paraformaldehyde. Then, the slides were incubated with 1% Triton X-100 for 5 min and then incubated with 50 μL/slide TUNEL reaction mixture for 1 h at 37 °C. After incubation, slides were washed 3 times, and nuclei were stained with DAPI. The images were captured using a fluorescence microscope. To calculate the apoptosis percentage, five high-power fields ($\times$400) were evaluated for TUNEL-positive cells in each group.

2.12 Statistical Analysis

All statistical tests were performed with SPSS 16.0 software (IBM, Chicago, IL, USA). Quantitative data were expressed as means $\pm$ SD of at least three independent experiments. Student's *t*-test compared results between two groups. One-way analysis of variance (ANOVA) was employed for the comparisons among multiple groups followed by Tukey's post hoc test. Significance was considered as $p < 0.05$.

3. Results

3.1 Albumin Overload Induced Mitochondrial Dysfunction and Mitophagy Activation in HK-2 Cells

We started our investigations by examining mitochondrial function during albumin overload treatment of HK-2 cells. As we know, a series of redox reactions creates an electrochemical gradient through the mitochondrial electron transport chain, which drives the synthesis of ATP and generates the mitochondrial membrane potential ($\Delta\psi$m). Therefore, we firstly measured the $\Delta\psi$m and ATP generation to evaluated mitochondrial function. The results revealed a clear decrease of $\Delta\psi$m (Fig. 1A,B) and ATP generation (Fig. 1C) in albumin overload-treated HK-2 cells, indicating mitochondrial dysfunction after albumin overload. Mitochondria, as the source of intracellular ROS, when confronting with oxidative stress, is the primary target attacked by ROS, and produces excessive amounts of ROS due to the damage to enzymes in the electron transport chain. Given this, we assessed the intracellular ROS by

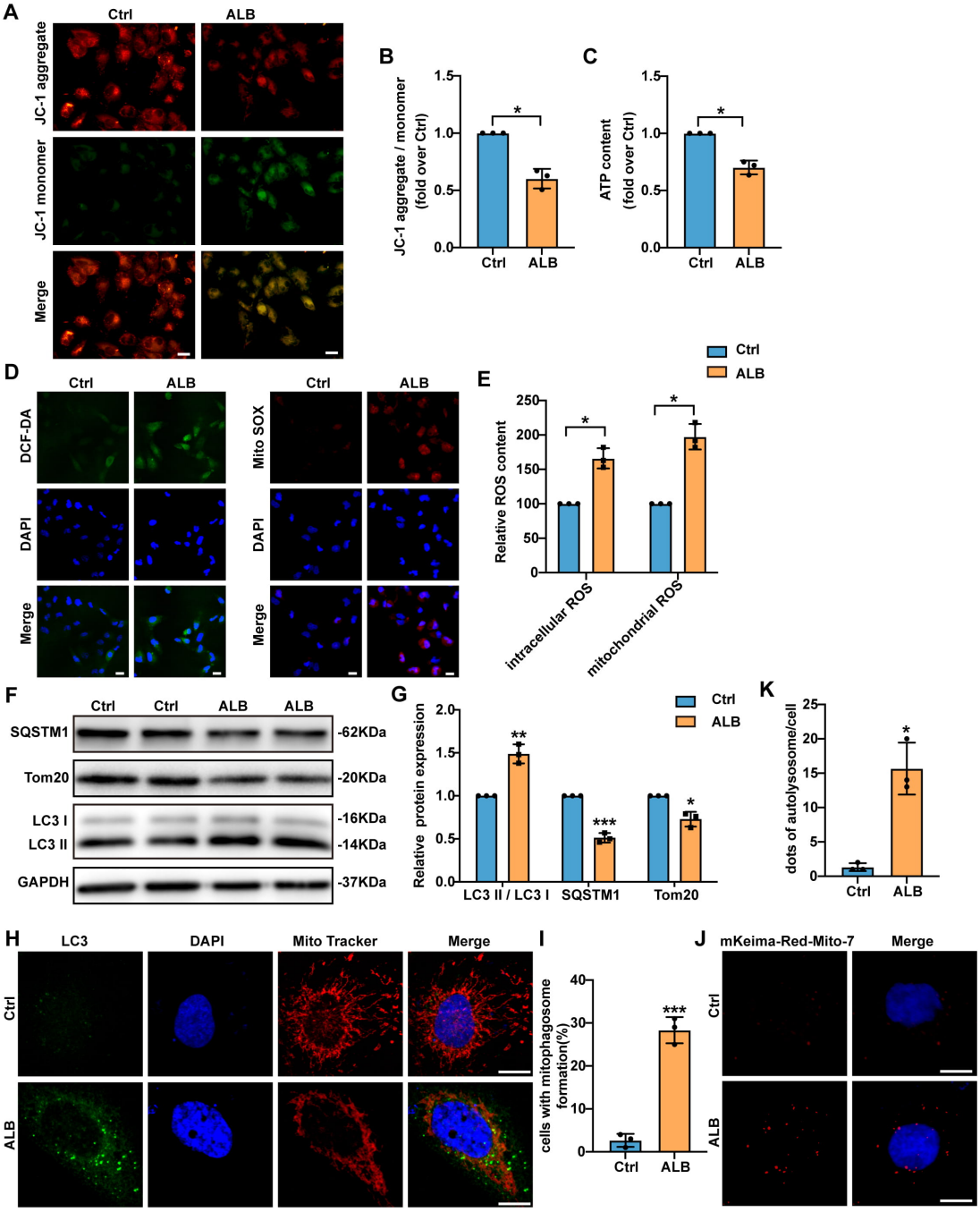

Fig. 1. Albumin overload induced mitochondrial dysfunction, ROS generation and mitophagy activation in HK-2 cells. (A) Representative images of JC-1 staining showing red fluorescence of JC-1 aggregate and green signal of monomer. Scale bar: 20 μm. (B) Quantification of the ratio of JC-1 aggregate to JC-1 monomer. (C) ATP contents. (D) Representative images of DCFH-DA staining for intracellular ROS and MitoSOX staining for mitochondrial ROS. Scale bar: 20 μm. (E) Quantification of DCFH-DA fluorescence intensity and MitoSOX fluorescence intensity. (F) Representative blots. (G) Densitometry of protein signals. (H) Representative images of mitophagy. Mitochondria were labeled with MitoTracker Red and autophagosomes were labeled with LC3 antibody. Scale bar: 10 μm. (I) Quantitative analysis of mitophagosome formation. (J) Representative images of autolysosomes formation. HK-2 cells were transfected with the mKeima-Red-Mito-7 plasmid, followed by treatment with 8 mg/mL albumin. The fluorescence was detected by confocal microscope. Scale bar = 10 μm. (K) Quantitative analysis of autolysosomes formation. Data are depicted as the mean $\pm$ SD from three independent experiments. *$p < 0.05$; **$p < 0.01$; ***$p < 0.001$. Ctrl, control; ALB, albumin.

DCFH-DA and mitochondrial ROS by MitoSOX Red staining respectively. The results showed that both intracellular ROS and mitochondrial ROS were increased by albumin overload (Fig. 1D,E).

We then examined the occurrence of mitophagy during albumin overload in HK-2 cells. Immunoblot analyses revealed that albumin overload induced the conversion of LC3-I to LC3-II and decreased the level of SQSTM1 (Fig. 1F,G), indicating autophagy activation. Immunoblot analyses confirmed that albumin overload induced a marked reduction in translocase of outer mitochondrial membrane 20 homolog (Tom20) (Fig. 1F,G), suggesting mitochondrial clearance by mitophagy. We then performed some direct observations of mitophagy by assessing mitophagosome formation following the colocalization of autophagosomes and mitochondria. These evaluations were performed by labeling mitochondrial with MitoTracker Red and autophagosome staining with a fluorescently labeled LC3 antibody (Fig. 1H). These evaluations revealed very few LC3 green-fluorescent puncta within the control cells, indicating a low level of autophagy. In contrast, albumin overload significantly increased the expression of LC3, indicating increased autophagosome formation. Notably, some LC3 green-fluorescent puncta colocalized with the Mito-Tracker signals in cells following albumin overload (Fig. 1H,I), indicating mitophagosome formation. To further confirm the occurrence of mitophagy, mito-Keima, a pH-sensitive fluorescent protein, was transfected into HK-2 cells to determine mitochondrial movement from the cytoplasm to the lysosome. As shown in Fig. 1J,K, red spots appeared in the cytoplasm upon albumin overload, indicating that mitochondria tended to form autolysosomes. These results confirmed the activation of autophagy and mitophagy during albumin overload in HK-2 cells.

3.2 The PINK1/Parkin-Dependent Mitophagy Pathway is Implicated in Albumin Overload-Induced Mitophagy

HK-2 cells exposed to albumin overload showed increased expression of PINK1, Parkin, and phospho-Parkin (Fig. 2A,B), indicating activation of the PINK1/Parkin-dependent mitophagy pathway. Given this, we determined the role of this pathway in these cells via the controlled inhibition of Parkin expression using Parkin siRNA transfection (Fig. 2C–E). There was a significant decrease in albumin overload-induced mitophagy and autolysosomes in Parkin siRNA-treated cells (Fig. 2F–I), which was accompanied by the partial restoration of Tom20 expression in these cells (Fig. 2A,B). Conversely, the overexpression of Parkin (Fig. 3A–E) further increased albumin overload-induced mitophagy and autolysosomes (Fig. 3F–I), as well as Tom20 degradation (Fig. 3D,E). Taken together, these results indicate that the PINK1/Parkin pathway critically contributes to tubular cell mitophagy in response to albumin overload.

3.3 Silencing of Parkin Aggravates Albumin Overload-Induced Mitochondrial Dysfunction in HK-2 Cells

Mitophagy plays an essential role in clearing damaged mitochondria. Therefore, mitophagy deficiency may allow the accumulation of damaged mitochondria, thereby impacting mitochondrial function. To determine the effect of PINK1/Parkin-mediated mitophagy on mitochondrial function, we first assessed the effect of Parkin silencing on $\Delta\psi$m, ATP generation, and ROS production during albumin overload in HK-2 cells. Under control conditions, $\Delta\psi$m loss and ROS production were at low levels in both control siRNA-transfected HK-2 cells and Parkin siRNA-transfected HK-2 cells (**Supplementary Fig. 1**). Silencing of Parkin further accelerated albumin overload-induced loss of $\Delta\psi$m (Fig. 4A,B). Consistently, silencing of Parkin aggravated the inhibitory effect of albumin overload on ATP production (Fig. 4C). Also, silencing of Parkin enhanced albumin overload-induced intracellular and mitochondrial ROS levels (Fig. 4D–G).

3.4 Overexpression of Parkin Attenuated Albumin Overload-Induced Mitochondrial Dysfunction

Given these results we went on to evaluate the effects of upregulating mitophagy via Parkin overexpression on albumin overload-induced mitochondrial dysfunction in HK-2 cells. Under control conditions, $\Delta\psi$m loss and ROS production were at low levels in both control plasmid empty vector-transfected HK-2 cells and Parkin overexpression plasmids-transfected HK-2 cells (**Supplementary Fig. 1**). Parkin overexpression alleviated the albumin overload-induced loss of $\Delta\Psi$m (Fig. 5A,B) and reduction in ATP levels (Fig. 5C). Consistently, Parkin overexpression inhibited albumin overload-induced intracellular and mitochondrial ROS generation in HK-2 cells (Fig. 5D–G). Thus, these results indicate the critical role of PINK1/Parkin-mediated mitophagy in the clearance of damaged mitochondria and protection of mitochondrial function during albumin overload in HK-2 cells.

3.5 Silencing of Parkin Aggravated Albumin Overload-Induced Apoptosis in HK-2 Cells

We then examined the effect of inhibiting mitophagy on apoptosis following albumin overload by silencing Parkin expression. Under control conditions, apoptosis rate and the expression of cleaved caspase 3 were at low levels in both control siRNA-transfected HK-2 cells and Parkin siRNA-transfected HK-2 cells (**Supplementary Fig. 2**). Upon albumin overload, many cells presented with nuclear morphology typical of apoptosis and were TUNEL-positive (Fig. 6A). Cell counting revealed that albumin overload induced apoptosis in ~17% of the control siRNA-transfected HK-2 cells, but this increased to ~25% in Parkin siRNA-transfected HK-2 cells (Fig. 6B). These results were confirmed by an immunoblot analysis that re-

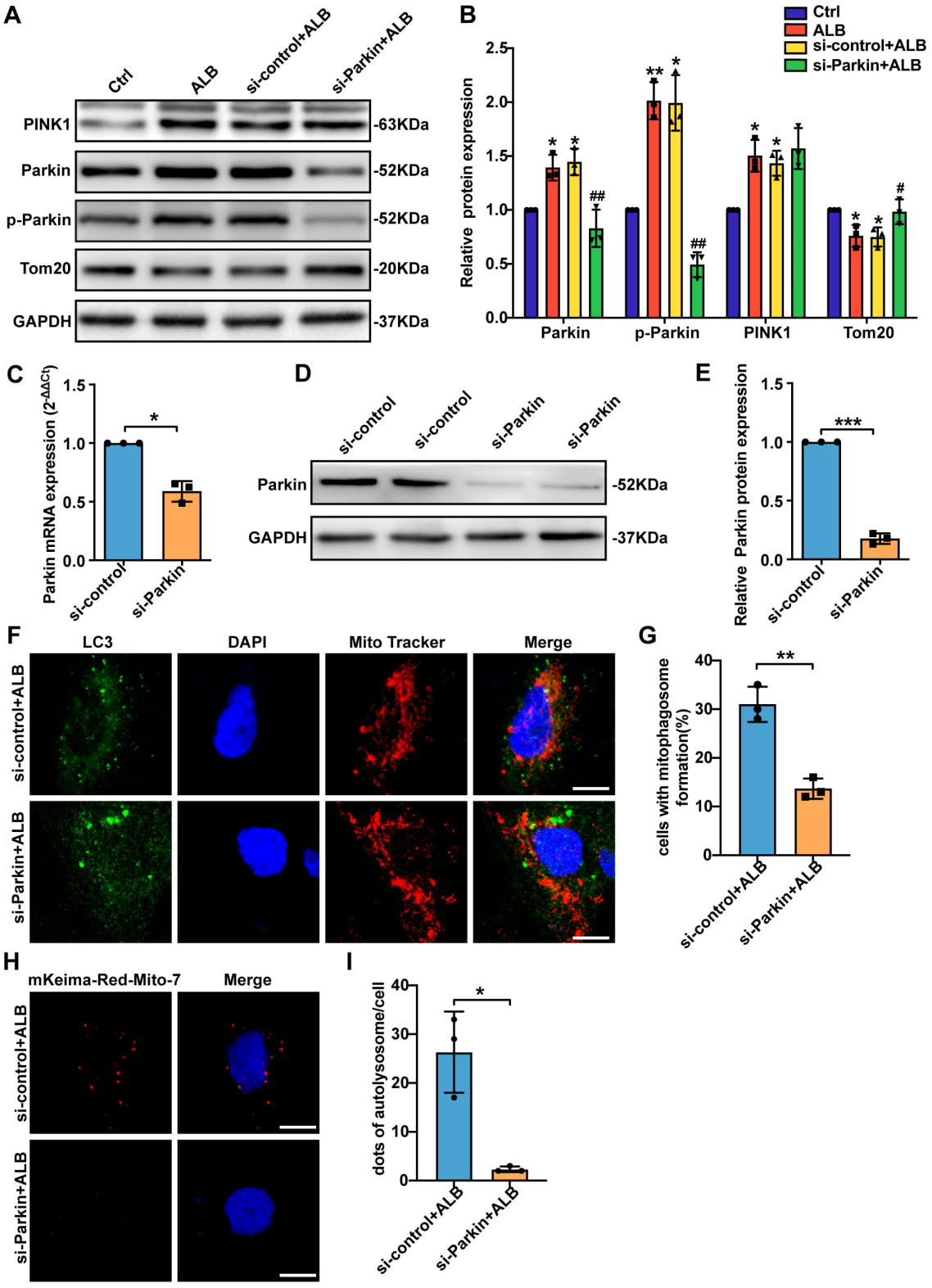

Fig. 2. Silencing of Parkin inhibited albumin overload-induced mitophagy in HK-2 cells. HK-2 cells were transfected with Parkin siRNA or control siRNA for 48 h followed by treatment with albumin (8 mg/mL) for 8 h. (A) Representative blots. (B) Densitometry of protein signals. *$p < 0.05$ vs. Ctrl; $^{\#}p < 0.05$ vs. si-control + ALB; $^{\#\#}p < 0.01$ vs. si-control + ALB. (C) Quantification of Parkin mRNA expression. * $p < 0.05$. (D) Representative blots. (E) Densitometry of protein signals. ***$p < 0.001$. (F) Representative images of mitophagy. Scale bar: 10 μm. (G) Quantitative analysis of mitophagosome formation. (H) Representative images of autolysosomes formation. Scale bar = 10 μm. (I) Quantitative analysis of autolysosomes formation. *$p < 0.05$, **$p < 0.01$. Data are depicted as the mean $\pm$ SD from three independent experiments. Ctrl, control; ALB, albumin; si-control, control siRNA; si-Parkin, Parkin siRNA.

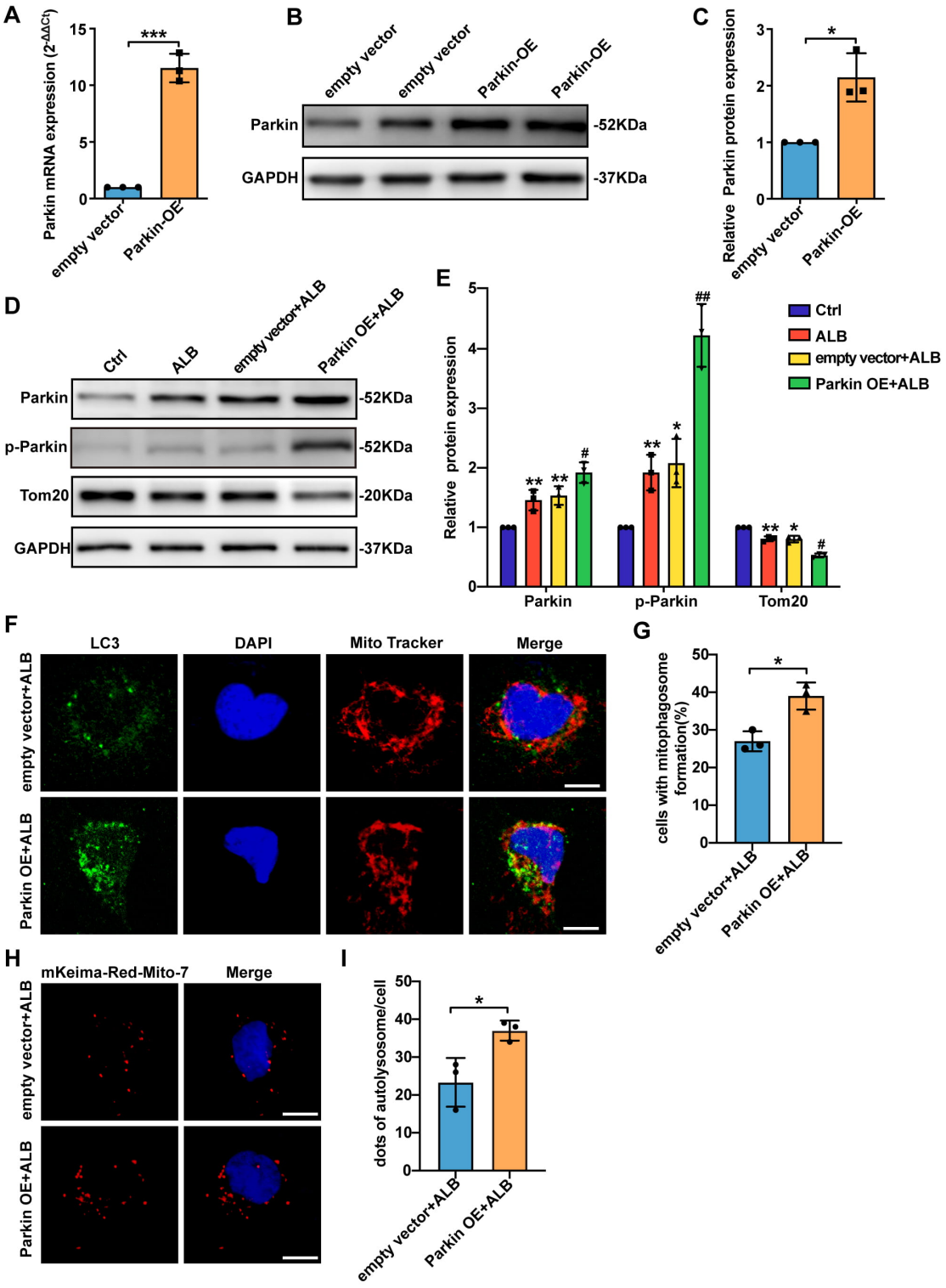

Fig. 3. Overexpression of Parkin enhanced albumin overload-induced mitophagy in HK-2 cells. HK-2 cells were transfected with Parkin overexpression plasmids or empty vector for 48 h followed by treatment with albumin (8 mg/mL) for 8 h. (A) Quantification of Parkin mRNA expression. ***$p < 0.001$. (B) Representative blots. (C) Densitometry of protein signals. *$p < 0.05$. (D) Representative blots. (E) Densitometry of protein signals. *$p < 0.05$ vs. Ctrl; **$p < 0.01$ vs. Ctrl; $^{\#}p < 0.05$ vs. empty vector + ALB. (F) Representative images of mitophagy. Scale bar: 10 μm. (G) Quantitative analysis of mitophagosome formation. (H) Representative images of autolysosomes formation. Scale bar = 10 μm. (I) Quantitative analysis of autolysosomes formation. *$p < 0.05$. Data are depicted as the mean $\pm$ SD from three independent experiments. Ctrl, control; ALB, albumin; empty vector, control empty plasmid vector; Parkin OE, Parkin overexpression plasmids.

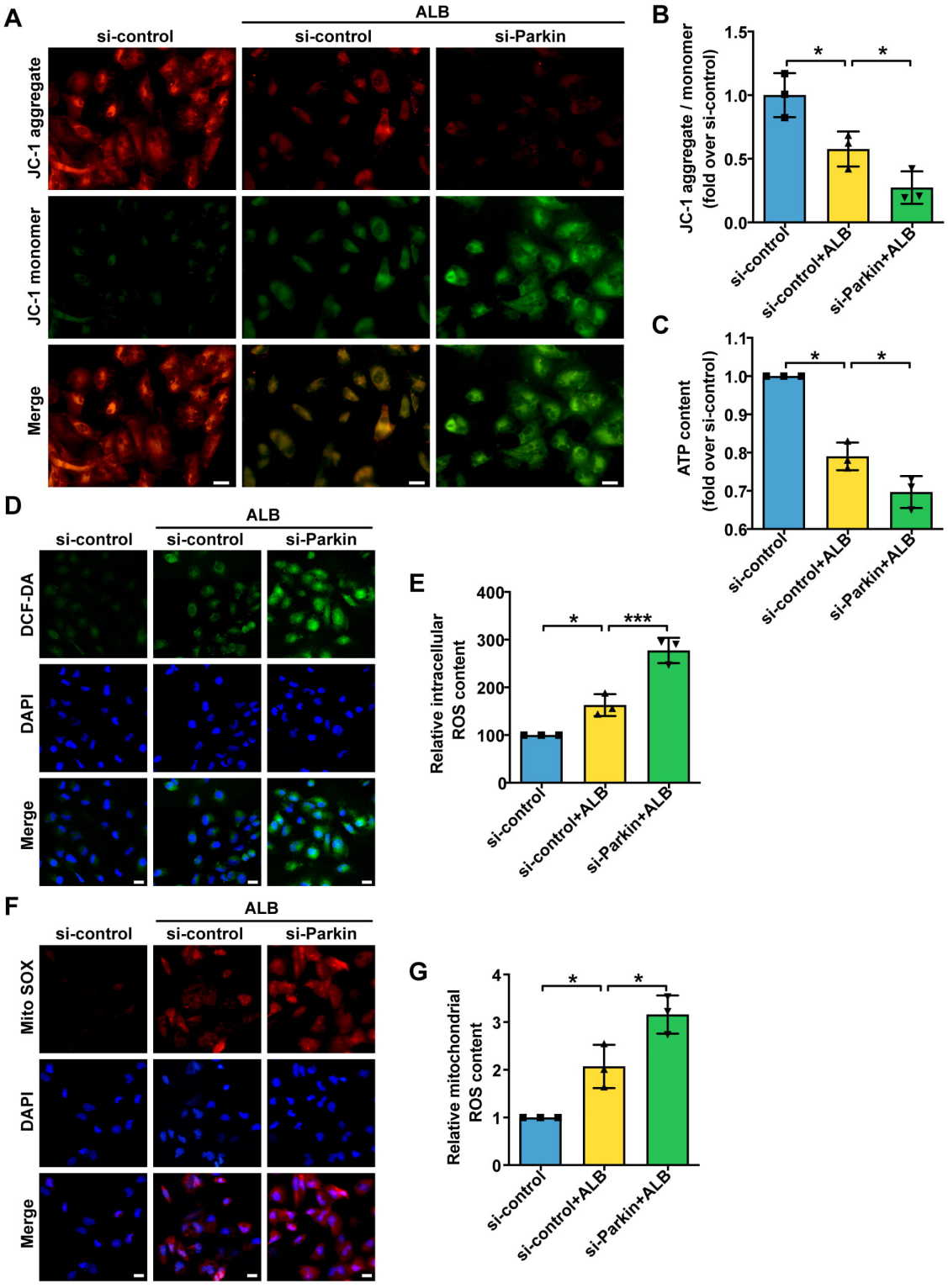

Fig. 4. Silencing of Parkin aggravated albumin overload-induced mitochondrial dysfunction and ROS generation. (A) Representative images of JC-1 staining showing red fluorescence of JC-1 aggregate and green signal of monomer. Scale bar: 20 μm. (B) Quantification of the ratio of JC-1 aggregate to JC-1 monomer. (C) ATP contents. (D) Representative images of DCFH-DA staining for intracellular ROS. Scale bar: 20 μm. (E) Quantification of DCFH-DA fluorescence intensity. (F) Representative images of MitoSOX staining for mitochondrial ROS. Scale bar: 20 μm. (G) Quantification of MitoSOX fluorescence intensity. Data are depicted as the mean $\pm$ SD from three independent experiments. *$p < 0.05$; ***$p < 0.001$. ALB, albumin; si-control, control siRNA; si-Parkin, Parkin siRNA.

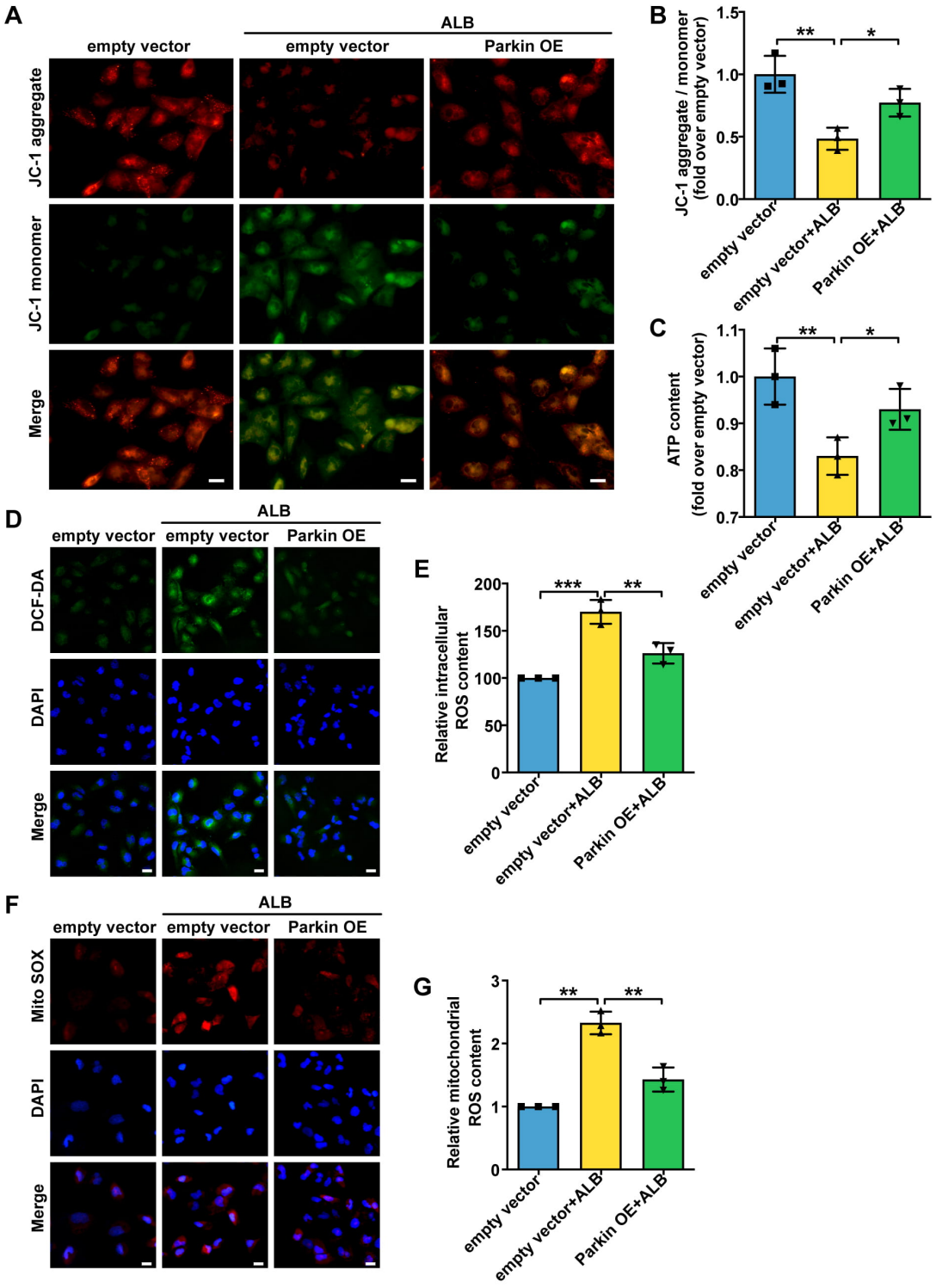

Fig. 5. Overexpression of Parkin attenuated albumin overload-induced mitochondrial dysfunction and ROS generation. (A) Representative images of JC-1 staining showing red fluorescence of JC-1 aggregate and green signal of monomer. Scale bar: 20 μm. (B) Quantification of the ratio of JC-1 aggregate to JC-1 monomer. (C) ATP contents. (D) Representative images of DCFH-DA staining for intracellular ROS. Scale bar: 20 μm. (E) Quantification of DCFH-DA fluorescence intensity. (F) Representative images of MitoSOX staining for mitochondrial ROS. Scale bar: 20 μm. (G) Quantification of MitoSOX fluorescence intensity. Data are depicted as the mean $\pm$ SD from three independent experiments. *$p < 0.05$; **$p < 0.01$; ***$p < 0.001$. ALB, albumin; empty vector, control empty plasmid vector; Parkin OE, Parkin overexpression plasmids.

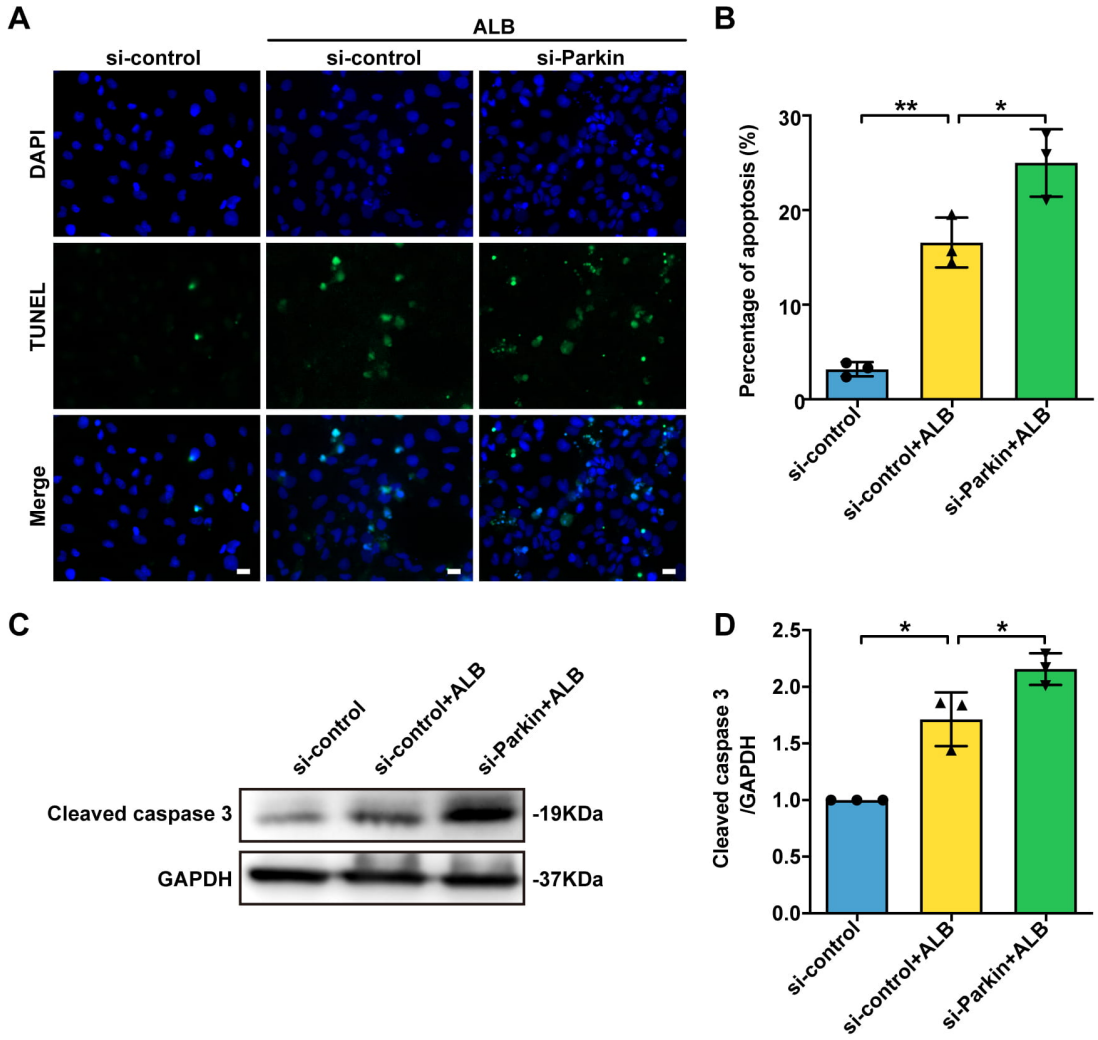

Fig. 6. Silencing of Parkin aggravated albumin overload-induced apoptosis in HK-2 cells. (A) Representative images of TUNEL staining of HK-2 cells. Scale bar: 20 μm. (B) Apoptosis percentage. (C) Whole-cell lysates were collected for western blotting analysis of cleaved caspase 3 and GAPDH (loading control). (D) Densitometry of cleaved caspase 3. Data are depicted as the mean $\pm$ SD from three independent experiments. *$p < 0.05$; **$p < 0.01$. ALB, albumin; si-control, control siRNA; si-Parkin, Parkin siRNA.

vealed a markedly increased expression of cleaved caspase 3 in Parkin siRNA-transfected cells compared to that in the control cells (Fig. 6C,D).

3.6 Overexpression of Parkin Attenuated Albumin Overload-Induced Apoptosis in HK-2 Cells

In contrast to mitophagy deficiency, the effect of the upregulation of mitophagy via Parkin overexpression on albumin overload-induced apoptosis was investigated. Under control conditions, apoptosis rate and the expression of cleaved caspase 3 were at low levels in both control plasmid empty vector-transfected HK-2 cells and Parkin overexpression plasmids-transfected HK-2 cells (**Supplementary Fig. 2**). In response to albumin overload, HK-2 cells with Parkin overexpression plasmids showed fewer TUNEL-positive cells (Fig. 7A,B) and lower levels of Cleaved caspase 3 than control plasmid empty vector cells (Fig. 7C,D). Collectively, these findings provide compelling evidence for the pro-survival role of PINK1/Parkin mediated mitophagy in albumin overload-induced HK-2 cell injury.

4. Discussion

Despite its clear importance, the role and mechanism of mitophagy in proteinuria-induced tubular damage remain unclear. Here, we demonstrated the mitochondrial dysfunction and the activation of mitophagy in tubular cells during albumin overload using an *in vitro* model. Tubular cell mitophagy following albumin overload was primarily mediated via the PINK1/Parkin pathway. Functionally, we showed that, by clearing damaged mitochondria and maintaining mitochondrial function, this mitophagy pathway contributed to tubular cell survival during albumin overload.

Urinary albumin is the major protein component of

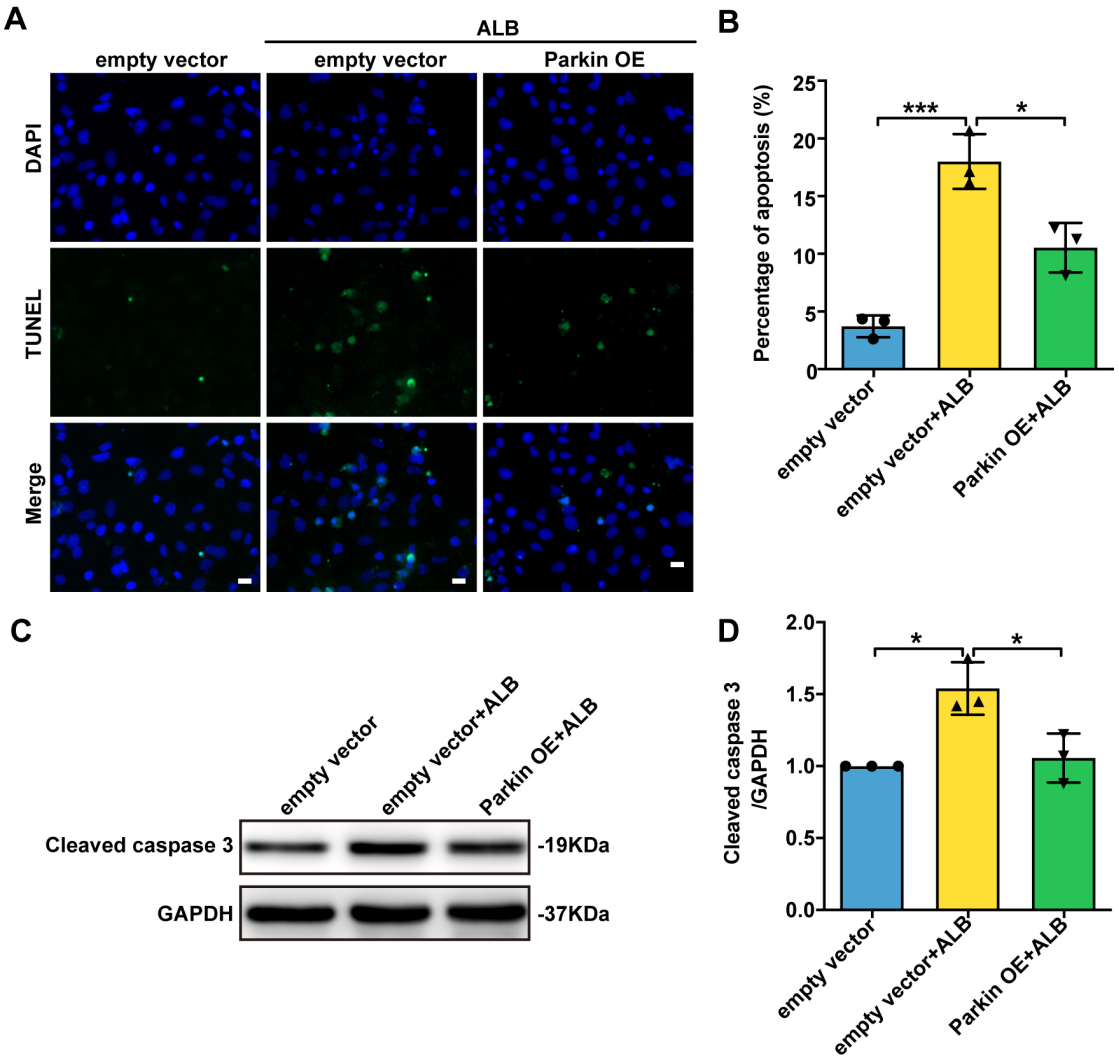

Fig. 7. Overexpression of Parkin attenuated albumin overload-induced apoptosis in HK-2 cells. (A) Representative images of TUNEL staining of HK-2 cells. Scale bar: 20 μm. (B) Apoptosis percentage. (C) Whole-cell lysates were collected for western blotting analysis of Cleaved caspase 3 and GAPDH (loading control). (D) Densitometry of Cleaved caspase 3. Data are depicted as the mean ± SD from three independent experiments. *$p < 0.05$; ***$p < 0.001$. ALB, albumin; empty vector, control empty plasmid vector; Parkin OE, Parkin overexpression plasmids.

nephrotic syndrome urine and is known to be highly toxic to renal tubular cells [19,20]. Mitochondrial dysfunction is considered an early pathophysiological indicator of these effects and may play a key role in albumin overload-induced tubular cell injury [9,21]. The albumin overload *in vitro* model established by treating renal tubular epithelial cells with 8-10mg/ml albumin for 8–24 h is widely used to study the effect of albumin on renal injury [5,21,22]. Previous and our present studies have confirmed significant changes in mitochondrial morphology, function, and ROS production in response to 8 mg/mL albumin treatment for 8 h [23]. In addition, our current study has provided evidence of mitophagy activation during 8 mg/mL albumin treatment for 8 h in tubular cells (Fig. 1). Many reports have suggested that mitochondrial depolarization and abnormal ROS production are necessary to promote mitophagy activation [21,24,25], and our results support this view.

The PINK1/Parkin-dependent mitophagy pathway is recognized as the major mitophagy pathway activated under cellular stress. PINK1 and Parkin double knockout cells reportedly do not demonstrate any additive effects on mitophagy following renal ischemia-reperfusion (I-R), indicating that PINK1 and Parkin work within a common mitophagy pathway in tubular cells [26]. Here, we found induction of the PINK1/Parkin pathway in renal tubular cells in an *in vitro* model of albumin overload (Fig. 2A,B). Furthermore, silencing of Parkin inhibited mitophagy during albumin overload (Fig. 2), while overexpression of Parkin further increased albumin overload-induced mitophagy (Fig. 3). These results suggest that

the PINK1/Parkin pathway is the major regulator for tubular cell mitophagy following albumin overload. Notably, there may be alternative mitophagy pathways where different proteins and lipids can recruit autophagic machinery without the involvement of PINK1 and Parkin [27]. Mitophagy receptors, such as Bcl-2 interacting protein 3 (BNIP3), BNIP3-like protein (BNIP3L/NIX), and FUN14 domain containing 1, can directly bind to LC3B, thereby inducing the activation of mitophagy [28–30]. Thus, multiple pathways regulating mitophagy may be activated in tubular cells under different pathological conditions. However, the PINK1/Parkin pathway remains the most well-studied pathway underlying mitophagy in kidney diseases.

An increase in data has allowed for a more nuanced evaluation of the functions of mitophagy in kidney diseases. Studies have described the protective effects of PINK/Parkin-mediated mitophagy in cisplatin-induced kidney injury and nephrotoxicity [17,31], while others have highlighted the fact that both BNIP3- and PINK1/Parkin-mediated mitophagy reduce mitochondrial damage and protect renal tubules during renal I-R injury [26,32]. Furthermore, the mitochondrial-targeting antioxidant, MitoQ, reversed mitophagy by upregulating the expression of PINK and Parkin, thereby preventing tubular injury in diabetic kidney disease in both *in vitro* and *in vivo* disease models [15]. We previously showed that inhibitors of autophagy enhanced albumin overload-induced mitochondrial injury, while autophagy activators induced protective effects, suggesting that autophagy may provide some protective effects during this disease [21]. Findings from the current study support this hypothesis. We found that inhibiting mitophagy via Parkin silencing accelerated albumin overload-induced mitochondrial dysfunction and elevated ROS production, leading to an increase in tubular cell injury (Figs. 4,6). Additionally, we showed that upregulation of mitophagy by Parkin overexpression ameliorated mitochondrial oxidative stress and dysfunction, which was accompanied by reduced apoptosis of the tubular cells following albumin overload (Figs. 5,7). Thus, our results suggest that the clearance of damaged mitochondria via PINK1/Parkin-mediated mitophagy is a valuable mechanism of renoprotection afforded by an autophagic process during albumin overload. Our results are consistent with a recent study showing that NIX-mediated mitophagy alleviates tubular apoptosis and renal damage caused by proteinuria [33]. Nevertheless, more research is needed to elucidate whether other signaling pathways are involved in regulating proteinuria-induced mitophagy in tubular cells.

5. Conclusions

In conclusion, this study provides substantial evidence for PINK1/Parkin-mediated mitophagy activation in renal tubular cells during albumin overload. It also supports the hypothesis that the clearing of damaged mitochondria via PINK1/Parkin-mediated mitophagy plays a vital role in maintaining mitochondrial function and reducing ROS production, thus protecting renal tubular cells during albumin overload. Overall, these findings suggest that upregulation of PINK1/Parkin-mediated mitophagy may be a potential therapeutic approach for alleviating proteinuria-induced renal tubular cell damage.

Author Contributions

QZ supervised the work; JT and PD designed the experiments with help from QZ; JT and PD performed the experiments; PD and YM wrote the manuscript; All authors discussed the results and commented on the manuscript. All authors provided critical comments on the manuscript. All authors approved the final version of the manuscript and agree to be accountable for all aspects of the work in ensuring that questions related to the accuracy or integrity of any part of the work are appropriately investigated and resolved. All persons designated as authors qualify for authorship, and all those who qualify for authorship are listed.

Ethics Approval and Consent to Participate

Not applicable.

Acknowledgment

Not applicable.

Funding

This work was supported by the Major Research Plan of the National Natural Science Foundation of China [grant number 92163213], and the General Program of the National Natural Science Foundation of China [grant number 81970085].

Conflict of Interest

The authors declare no conflict of interest.

Supplementary Material

Supplementary material associated with this article can be found, in the online version, at https://doi.org/10.31083/j.fbl2706184.

References

[1] Abbate M, Zoja C, Remuzzi G. How does proteinuria cause progressive renal damage? Journal of the American Society of Nephrology. 2006; 17: 2974–2984.

[2] Kinashi H, Falke LL, Nguyen TQ, Bovenschen N, Aten J, Leask A, *et al*. Connective tissue growth factor regulates fibrosis-associated renal lymphangiogenesis. Kidney International. 2017; 92: 850–863.

[3] Wong DWL, Yiu WH, Wu HJ, Li RX, Liu Y, Chan KW, *et al*. Downregulation of renal tubular Wnt/β-catenin signaling by Dickkopf-3 induces tubular cell death in proteinuric nephropathy. Cell Death & Disease. 2016; 7: e2155.

[4] Deng J, Zhang X, Wu H, Gan Y, Ye L, Zheng H, *et al*. ROS-ERK Pathway as Dual Mediators of Cellular Injury and Autophagy-Associated Adaptive Response in Urinary Protein-Irritated Re-

nal Tubular Epithelial Cells. Journal of Diabetes Research. 2021; 2021: 6614848.

[5] Zhuang Y, Ding G, Zhao M, Bai M, Yang L, Ni J, *et al*. NLRP3 Inflammasome Mediates Albumin-induced Renal Tubular Injury through Impaired Mitochondrial Function. Journal of Biological Chemistry. 2014; 289: 25101–25111.

[6] Liu WJ, Xu B, Ye L, Liang D, Wu H, Zheng Y, *et al*. Urinary proteins induce lysosomal membrane permeabilization and lysosomal dysfunction in renal tubular epithelial cells. American Journal of Physiology-Renal Physiology. 2015; 308: F639–F649.

[7] Mishra P, Chan DC. Metabolic regulation of mitochondrial dynamics. Journal of Cell Biology. 2016; 212: 379–387.

[8] Hsu WH, Hua KF, Tuan LH, Tsai YL, Chu LJ, Lee YC, *et al*. Compound K inhibits priming and mitochondria-associated activating signals of NLRP3 inflammasome in renal tubulointerstitial lesions. Nephrology Dialysis Transplantation. 2020; 35: 74–85.

[9] Erkan E, Devarajan P, Schwartz GJ. Mitochondria are the Major Targets in Albumin-Induced Apoptosis in Proximal Tubule Cells. Journal of the American Society of Nephrology. 2007; 18: 1199–1208.

[10] Gumeni S, Trougakos IP. Cross Talk of Proteostasis and Mitostasis in Cellular Homeodynamics, Ageing, and Disease. Oxidative Medicine and Cellular Longevity. 2016; 2016: 4587691.

[11] Li W, Cheng H, Li G, Zhang L. Mitochondrial Damage and the Road to Exhaustion. Cell Metabolism. 2020; 32: 905–907.

[12] Matsuda N, Sato S, Shiba K, Okatsu K, Saisho K, Gautier CA, *et al*. PINK1 stabilized by mitochondrial depolarization recruits Parkin to damaged mitochondria and activates latent Parkin for mitophagy. Journal of Cell Biology. 2010; 189: 211–221.

[13] Geisler S, Holmström KM, Skujat D, Fiesel FC, Rothfuss OC, Kahle PJ, *et al*. PINK1/Parkin-mediated mitophagy is dependent on VDAC1 and p62/SQSTM1. Nature Cell Biology. 2010; 12: 119–131.

[14] Kane LA, Lazarou M, Fogel AI, Li Y, Yamano K, Sarraf SA, *et al*. PINK1 phosphorylates ubiquitin to activate Parkin E3 ubiquitin ligase activity. Journal of Cell Biology. 2014; 205: 143–153.

[15] Xiao L, Xu X, Zhang F, Wang M, Xu Y, Tang D, *et al*. The mitochondria-targeted antioxidant MitoQ ameliorated tubular injury mediated by mitophagy in diabetic kidney disease via Nrf2/PINK1. Redox Biology. 2017; 11: 297–311.

[16] Kimura T, Isaka Y, Yoshimori T. Autophagy and kidney inflammation. Autophagy. 2017; 13: 997–1003.

[17] Zhao C, Chen Z, Xu X, An X, Duan S, Huang Z, *et al*. Pink1/Parkin-mediated mitophagy play a protective role in cisplatin induced renal tubular epithelial cells injury. Experimental Cell Research. 2017; 350: 390–397.

[18] Liu WJ, Luo M, Tan J, Chen W, Huang L, Yang C, *et al*. Autophagy activation reduces renal tubular injury induced by urinary proteins. Autophagy. 2014; 10: 243–256.

[19] Gorriz JL, Martinez-Castelao A. Proteinuria: detection and role in native renal disease progression. Transplantation Reviews. 2012; 26: 3–13.

[20] Li X, Pabla N, Wei Q, Dong G, Messing RO, Wang CY, *et al*. PKC-delta promotes renal tubular cell apoptosis associated with proteinuria. Journal of the American Society of Nephrology. 2010; 21: 1115–1124.

[21] Tan J, Wang M, Song S, Miao Y, Zhang Q. Autophagy activation promotes removal of damaged mitochondria and protects against renal tubular injury induced by albumin overload. Histology & Histopathology. 2018; 33: 681–690.

[22] Delitsikou V, Jarad G, Rajaram RD, Ino F, Rutkowski JM, Chen C, *et al*. Klotho regulation by albuminuria is dependent on ATF3 and endoplasmic reticulum stress. The FASEB Journal. 2020; 34: 2087–2104.

[23] Nishi Y, Satoh M, Nagasu H, Kadoya H, Ihoriya C, Kidokoro K, *et al*. Selective estrogen receptor modulation attenuates proteinuria-induced renal tubular damage by modulating mitochondrial oxidative status. Kidney International. 2013; 83: 662–673.

[24] Zhang Y, Xi X, Mei Y, Zhao X, Zhou L, Ma M, *et al*. High-glucose induces retinal pigment epithelium mitochondrial pathways of apoptosis and inhibits mitophagy by regulating ROS/PINK1/Parkin signal pathway. Biomedicine & Pharmacotherapy. 2019; 111: 1315–1325.

[25] Jiang X, Chen X, Hua W, He J, Liu T, Li X, *et al*. PINK1/Parkin mediated mitophagy ameliorates palmitic acid-induced apoptosis through reducing mitochondrial ROS production in podocytes. Biochemical and Biophysical Research Communications. 2020; 525: 954–961.

[26] Tang C, Han H, Yan M, Zhu S, Liu J, Liu Z, *et al*. PINK1-PRKN/PARK2 pathway of mitophagy is activated to protect against renal ischemia-reperfusion injury. Autophagy. 2018; 14: 880–897.

[27] Terešak P, Lapao A, Subic N, Boya P, Elazar Z, Simonsen A. Regulation of PRKN-independent mitophagy. Autophagy. 2022; 18: 24–39.

[28] Sandoval H, Thiagarajan P, Dasgupta SK, Schumacher A, Prchal JT, Chen M, *et al*. Essential role for Nix in autophagic maturation of erythroid cells. Nature. 2008; 454: 232–235.

[29] Liu L, Feng D, Chen G, Chen M, Zheng Q, Song P, *et al*. Mitochondrial outer-membrane protein FUNDC1 mediates hypoxia-induced mitophagy in mammalian cells. Nature Cell Biology. 2012; 14: 177–185.

[30] Zhang H, Bosch-Marce M, Shimoda LA, Tan YS, Baek JH, Wesley JB, *et al*. Mitochondrial Autophagy is an HIF-1-dependent Adaptive Metabolic Response to Hypoxia. Journal of Biological Chemistry. 2008; 283: 10892–10903.

[31] Wang Y, Tang C, Cai J, Chen G, Zhang D, Zhang Z, *et al*. PINK1/Parkin-mediated mitophagy is activated in cisplatin nephrotoxicity to protect against kidney injury. Cell Death & Disease. 2018; 9: 1113.

[32] Ishihara M, Urushido M, Hamada K, Matsumoto T, Shimamura Y, Ogata K, *et al*. Sestrin-2 and BNIP3 regulate autophagy and mitophagy in renal tubular cells in acute kidney injury. American Journal of Physiology-Renal Physiology. 2013; 305: F495–F509.

[33] Xu D, Chen P, Wang B, Wang Y, Miao N, Yin F, *et al*. NIX-mediated mitophagy protects against proteinuria-induced tubular cell apoptosis and renal injury. The American Journal of Physiology-Renal Physiology. 2019; 316: F382–F395.